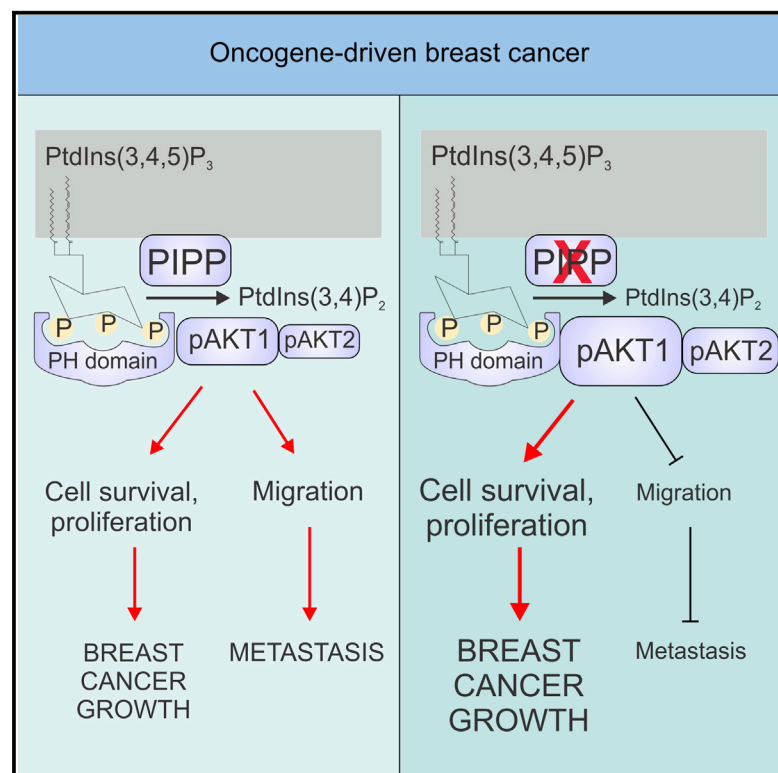Article

The Inositol Polyphosphate 5-Phosphatase PIPP Regulates AKT1-Dependent Breast Cancer Growth and Metastasis

Graphical Abstract

Authors

Lisa M. Ooms, Lauren C. Binge, Elizabeth M. Davies, ..., Paul Timpson, Catriona A. McLean, Christina A. Mitchell

Correspondence

christina.mitchell@monash.edu

In Brief

Ooms et al. identify the inositol polyphosphate 5-phosphatase PIPP as a suppressor of oncogenic PI3K/AKT signaling in breast cancer. PIPP depletion increases transformation and accelerates oncogene-driven tumor growth in vivo, while paradoxically reducing cell migration, invasion, and metastasis.

Highlights

- *Pipp* knockout promotes oncogene-driven breast cancer initiation and growth

- Ablation of *Pipp* impairs metastasis in a mouse model of breast cancer

- PIPP regulates AKT1-dependent cell migration and invasion

- Low *PIPP* expression is associated with ER-negative breast cancer and poor prognosis

CrossMark

CellPress

CellPress

The Inositol Polyphosphate 5-Phosphatase PIPP Regulates AKT1-Dependent Breast Cancer Growth and Metastasis

Lisa M. Ooms,[1,5] Lauren C. Binge,[1,5] Elizabeth M. Davies,[1] Parvin Rahman,[1] James R.W. Conway,[2] Rajendra Gurung,[1] Daniel T. Ferguson,[1] Antonella Papa,[1] Clare G. Fedele,[1,6] Jessica L. Vieusseux,[1,7] Ryan C. Chai,[1] Frank Koentgen,[3] John T. Price,[1,8] Tony Tiganis,[1] Paul Timpson,[2] Catriona A. McLean,[4] and Christina A. Mitchell[1,*]
[1]Department of Biochemistry and Molecular Biology, Monash University, Clayton, VIC 3800, Australia
[2]Garvan Institute of Medical Research, The Kinghorn Cancer Centre, Faculty of Medicine, St Vincent's Clinical School, University of NSW, Darlinghurst, NSW 2010, Australia
[3]Ozgene Pty Ltd, Bentley DC, WA 6983, Australia
[4]Department of Anatomical Pathology, Alfred Hospital, Prahran, VIC 3181, Australia
[5]Co-first author
[6]Present address: Melanoma Research Laboratory, Peter MacCallum Cancer Centre, East Melbourne, VIC 3002, Australia
[7]Present address: Metastasis Research Laboratory, Peter MacCallum Cancer Centre, East Melbourne, VIC 3002, Australia
[8]Present address: College of Health and Biomedicine, Victoria University, St Albans, VIC 3021, Australia
*Correspondence: christina.mitchell@monash.edu
http://dx.doi.org/10.1016/j.ccell.2015.07.003

SUMMARY

Metastasis is the major cause of breast cancer mortality. Phosphoinositide 3-kinase (PI3K) generated PtdIns(3,4,5)P_3 activates AKT, which promotes breast cancer cell proliferation and regulates migration. To date, none of the inositol polyphosphate 5-phosphatases that inhibit PI3K/AKT signaling have been reported as tumor suppressors in breast cancer. Here, we show depletion of the inositol polyphosphate 5-phosphatase PIPP (*INPP5J*) increases breast cancer cell transformation, but reduces cell migration and invasion. *Pipp* ablation accelerates oncogene-driven breast cancer tumor growth in vivo, but paradoxically reduces metastasis by regulating AKT1-dependent tumor cell migration. *PIPP* mRNA expression is reduced in human ER-negative breast cancers associated with reduced long-term outcome. Collectively, our findings identify PIPP as a suppressor of oncogenic PI3K/AKT signaling in breast cancer.

INTRODUCTION

In response to growth factor stimulation, activated class 1 phosphoinositide 3-kinase (PI3K) generates phosphatidylinositol 3,4,5-trisphosphate (PtdIns(3,4,5)P_3) that facilitates the activation of many effectors, including the serine/threonine kinase AKT (Miller et al., 2011; Yuan and Cantley, 2008). PI3K/AKT signaling drives cell proliferation and survival. *PIK3CA*, the gene that encodes the catalytic (p110α) subunit of class 1 PI3K, is mutated and activated in ∼35%–45% of luminal A (ER-positive (ER$^+$) and/or PR$^+$) and 29% of luminal B (ER$^+$ and/or

PR$^+$, HER2$^{+/-}$) breast cancers (Sabine et al., 2014; Cancer Genome Atlas Network, 2012). Transgenic overexpression of mutant *Pik3ca* or endogenous knock in of *Pik3ca*^{H1047R} in murine mammary glands leads to the spontaneous development of breast tumors (Liu et al., 2011; Meyer et al., 2011; Tikoo et al., 2012). Many PI3K mutations that occur in cancer are associated with poor outcomes, however, in breast cancer, the prognostic role of *PIK3CA* mutations is still emerging. Indeed, for reasons that remain unclear, expression of some *PIK3CA* mutants in luminal tumors may be associated with improved long-term survival (Dumont et al., 2012; Kalinsky et al., 2009).

Significance

Breast cancer is the most common cancer in women. Despite advances in treatments, many patients develop metastatic disease, the leading cause of breast cancer death. The phosphoinositide 3-kinase signaling pathway is frequently hyperactivated in breast cancer and represents a significant target for novel therapies. Here, we show that loss of *Pipp*, a negative regulator of PI3K signaling, promotes oncogene-driven breast cancer initiation and growth, but impairs metastasis. *PIPP* mRNA expression is decreased in ER-negative primary breast cancers associated with reduced relapse-free and overall survival. Our studies suggest that analysis of *PIPP* expression in human breast cancers may identify a subset of patients that would benefit from therapies targeting the PI3K signaling pathway.
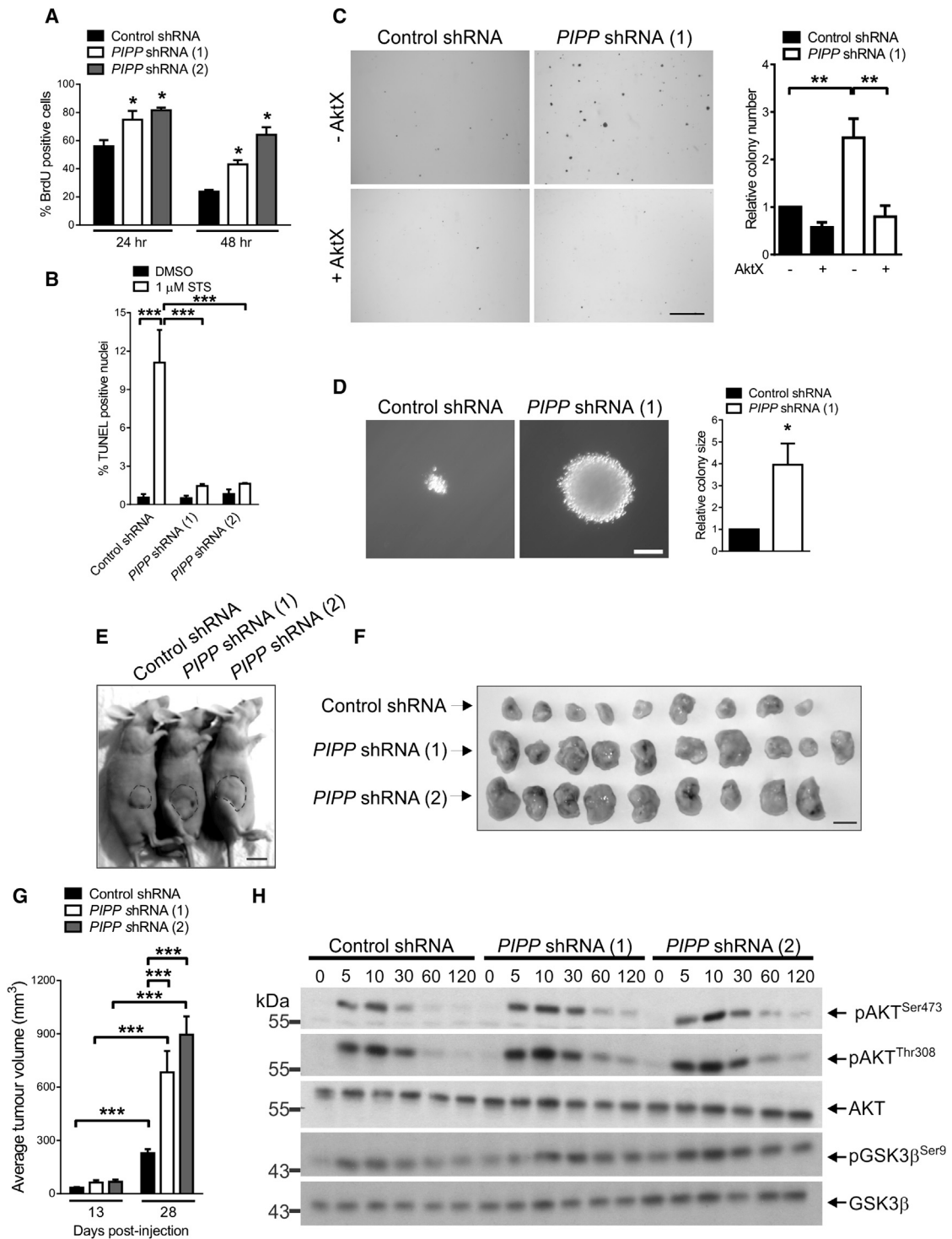
Figure 1. *PIPP* Depletion Enhances Cell Proliferation, Survival, and Tumorigenic Potential

(A) Control shRNA, *PIPP* shRNA (1), and (2) expressing MDA-MB-231 cells were serum-starved for 24 hr or 48 hr. The BrdU incorporation was assessed as a marker of cell proliferation. The data represent the average percentage of BrdU positive cells ± SEM, n = 4.

(B) MDA-MB-231 cells expressing control or *PIPP* shRNA (1) or *PIPP* shRNA (2) were grown in serum for 24 hr then treated with 1 μM staurosporine (STS) or DMSO for 6 hr. The apoptotic cells were identified by TUNEL staining. The data represent mean TUNEL positive nuclei ± SEM, n = 3.

(C) Control and *PIPP* shRNA (1) expressing MDA-MB-231 cells were suspended in soft agar ± the pan-AKT inhibitor AktX (5 μM) to assess anchorage independent cell growth. The number of colonies/well relative to untreated control shRNA expressing cells ± SEM was determined from five experiments performed in triplicate.

(legend continued on next page)

PI3K signaling is terminated by phosphoinositide phosphatases, such as the tumor suppressor PTEN, which hydrolyzes PtdIns(3,4,5)P_3 to form PtdIns(4,5)P_2 and thereby suppresses AKT activation. Germline mutations in PTEN in Cowden's syndrome are associated with a 25%–50% lifetime risk of breast cancer (Hollander et al., 2011). In addition, PTEN loss is observed in 30%–40% of sporadic cases of breast cancer associated with AKT hyperactivation and tumor progression (Zhang et al., 2013). Interestingly, an alternative pathway for the termination of PI3K signaling is mediated by inositol polyphosphate 5-phosphatases (5-phosphatase), which degrade PtdIns(3,4,5)P_3 to form PtdIns(3,4)P_2, and in turn 4-phosphatases, such as INPP4B, hydrolyze PtdIns(3,4)P_2 to form PI(3)P (Astle et al., 2007; Ooms et al., 2009). Although INPP4B is a potential tumor suppressor, to date there is no evidence that any of the ten mammalian 5-phosphatases suppress oncogenic PI3K/AKT signaling in breast cancer.

The proline rich inositol polyphosphate 5-phosphatase, PIPP, dephosphorylates PtdIns(3,4,5)P_3 to suppress AKT activation and oppose oncogenic PI3K signaling in cultured fibroblasts (Denley et al., 2009; Ooms et al., 2006). The gene encoding human PIPP (*INPP5J*) is located on chromosome 22q12. Allelic loss of chromosome 22q12 occurs in ~30% of breast tumors (Ellsworth et al., 2003; Iida et al., 1998; Osborne and Hamshere, 2000) and loss of heterozygosity (LOH) of chromosome 22q is frequent in breast carcinomas (Castells et al., 2000; Ellsworth et al., 2003; Iida et al., 1998). LOH of D22S1150 and D22S280, which map to either side of the *PIPP* gene, has been detected in 41 and 45% of breast carcinomas, respectively (Allione et al., 1998). In addition, *PIPP* mRNA expression is decreased in estrogen receptor-negative (ER⁻) breast cancers compared to ER⁺ tumors (Gruvberger et al., 2001; van 't Veer et al., 2002). However, whether PIPP acts as a tumor suppressor in regulating breast tumor growth, metastasis, and long-term survival has not been reported. In this study, we examined the role PIPP plays in breast cancer progression.

RESULTS

Decreased *PIPP* Expression Promotes Cell Proliferation and Survival

To investigate PIPP regulation of breast cancer cell proliferation and tumor growth, stable *PIPP* short hairpin (sh)RNA-mediated knockdown was undertaken in the ER⁻ MDA-MB-231 human breast cancer cell line. There were two distinct *PIPP*-specific shRNAs (*PIPP* shRNA [1] and [2]; Figure S1A) that resulted in ~45%–55% and ~60%–70% knockdown of *PIPP* mRNA expression, respectively, as assessed by quantitative RT-PCR (Figure S1B) and immunoblotting (Figure S1C). *PIPP* shRNA

knockdown enhanced cell proliferation (1.3–1.7-fold) under conditions of serum-starvation (24–48 hr) (Figure 1A), but had no effect on the proliferation of MDA-MB-231 cells grown in serum (Figure S1D). *PIPP* depletion was associated with decreased apoptosis (~6.8–7.7-fold) in response to staurosporine treatment (Figure 1B). The decrease in apoptosis was rescued by transient overexpression of exogenous wild-type, but not catalytically inactive shRNA-resistant HA-PIPP (Figure S1E), consistent with the inhibition of apoptosis by PIPP being dependent on its 5-phosphatase activity. The ability of cells to exhibit anchorage independent cell growth in soft agar is a feature of cell transformation. *PIPP* shRNA promoted anchorage independent cell growth with a significant increase in both the size (~4-fold) and number of colonies (~2.5-fold) formed compared to control cells (Figures 1C and 1D). To assess whether PIPP regulates breast cancer growth in vivo, MDA-MB-231-luc cells expressing *PIPP* or control shRNA were injected into the mammary fat pads of athymic nude mice and tumor growth was measured over 4 weeks. *PIPP* knockdown increased tumor size 2.6–3.3-fold compared to vector controls (Figures 1E–1G).

Activated AKT drives cell proliferation and inhibits apoptosis via phosphorylation of downstream effectors, such as GSK3β. *PIPP* shRNA knockdown increased phospho-AKT^Ser473 (pAKT^Ser473) and pAKT^Thr308 relative to total AKT and phospho-GSK3β^Ser9/GSK3β following epidermal growth factor (EGF) stimulation, suggesting PIPP suppresses AKT signaling in breast cancer cells (Figure 1H). In addition, *PIPP* shRNA knockdown increased phosphorylation of PRAS40 and other immunoreactive proteins detected by a phospho-AKT substrate antibody (Ivetac et al., 2009) (Figure S1F). The increased phosphorylation of AKT and AKT substrates in *PIPP* shRNA cells was suppressed by treatment with the PI3K inhibitor BKM120 (Figure S1F). Furthermore, the increased soft agar colony formation observed with *PIPP* knockdown was inhibited by the pan-AKT inhibitor, AktX (Figure 1C). Therefore, *PIPP* depletion promotes breast cancer cell proliferation, survival, and transformation in vitro and tumor growth in a xenograft mouse model.

To confirm the effects of *PIPP* depletion on ER⁻ breast cancer cells, *PIPP* knockdown was also undertaken in the triple negative breast cancer cell line, Hs578T, resulting in ~65% *PIPP* knockdown as assessed by quantitative RT-PCR (Figure S1G). *PIPP* shRNA knockdown enhanced cell proliferation (2.0–2.3-fold) under conditions of serum-starvation (Figure S1H) and increased the number of colonies formed (1.7-fold) in anchorage independent cell growth assays (Figure S1I). In addition, *PIPP* shRNA knockdown increased pAKT^Ser473 relative to total AKT following EGF stimulation (Figure S1J), consistent with the effects observed with *PIPP* depletion in MDA-MB-231 triple negative breast cancer cells.

(D) Mean colony size of *PIPP* shRNA (1) expressing MDA-MB-231 cells suspended in soft agar relative to control shRNA expressing cells ± SEM was determined from three experiments performed in triplicate.

(E–G) MDA-MB-231-luc cells expressing control or *PIPP*-specific shRNAs were injected into the mammary fat pads of athymic BALB/c nude mice and tumor growth assessed over 4 weeks. The imaging of tumors in vivo (E) and ex vivo (F) and quantification of tumor volume by calliper measurements (G) revealed *PIPP* shRNA knockdown cells formed larger tumors in vivo. The average tumor volumes from control shRNA (n = 9), *PIPP* shRNA (1) (n = 10), and *PIPP* shRNA (2) (n = 9) ± SEM are shown.

(H) MDA-MB-231 cells expressing control, *PIPP* shRNA (1), or *PIPP* shRNA (2) were serum-starved overnight then stimulated with 20 ng/ml EGF for the indicated times (min). The lysates were immunoblotted with antibodies specific for pAKT^Ser473, pAKT^Thr308, pGSK3β^Ser9, or total AKT or GSK3β as loading controls. The blots are representative of four experiments. The scale bars represent 2 mm (C), 500 μm (D), and 10 mm (E and F) (*p < 0.05, **p < 0.01, and ***p < 0.001). See also Figure S1.

Loss of *Pipp* Does Not Affect Mammary Gland Development

To assess the role PIPP plays in mammary development and tumorigenesis in vivo, we generated mice with a *Pipp* allele in which the second exon was flanked with *loxP* recombination sites (*Pipp^{fl/fl}*). The phenotype of *Pipp* knockout mice has not been reported to date. *Pipp^{fl/fl}* mice were crossed with CMV-*Cre* mice, resulting in *Pipp* deletion in all tissues (Figure S2). Absence of *Pipp* mRNA expression was shown by quantitative RT-PCR (Figure 2A). *Pipp^{−/−}* mice were viable and born at the expected Mendelian frequency. *Pipp^{−/−}* mice were fertile and displayed no overt phenotype at 4 months of age. PI3K/AKT signaling contributes to mammary gland morphogenesis, however, *Pipp^{−/−}* mammary glands (4 and 7 weeks) exhibited no abnormalities in terminal end bud number, ductal branching, morphology, or outgrowth into the mammary fat pad (Figures 2B–2D), suggesting that *Pipp* expression is not essential for murine mammary gland development. The outer layer of CK14 positive basal cells and inner layer of CK18 positive luminal epithelial cells within the ducts were unchanged in *Pipp^{−/−}* breast tissue (Figures 2E and 2F). Transgenic mice expressing constitutively active AKT or mice with conditional loss of *Pten* in the mammary gland exhibit delayed mammary gland involution following weaning (Li et al., 2002; Schwertfeger et al., 2001). At day 2 of involution, alveolar structures were apparent in wild-type and *Pipp^{−/−}* mice (Figure 2G). By day 5 of involution, alveolar structures were collapsed and adipocytes reappeared equally irrespective of *Pipp* expression, suggesting that PIPP does not regulate involution (Figure 2G). *Pik3ca* expression or loss of *Pten* leads to spontaneous mammary tumor formation in mice (Liu et al., 2011; Meyer et al., 2011; Tikoo et al., 2012). However, *Pipp^{−/−}* mice showed no evidence of mammary gland hyperplasia at 1 year of age (n = 8) (Figure 2H) or mammary tumors up to 20 months of age (*Pipp^{+/+}* n = 4 and *Pipp^{−/−}* n = 14). Therefore, loss of *Pipp* expression by itself in murine mammary tissue does not affect mammary gland development or promote initiation of de novo breast cancer.

PIPP Regulates Oncogene-Driven Breast Cancer Initiation and Primary Tumor Progression

As murine *Pipp* ablation per se did not lead to spontaneous mammary tumors, we investigated the consequences of loss of this 5-phosphatase in an oncogene-driven mammary cancer mouse model. Polyoma middle T (PyMT) oncogene expression in mammary epithelium leads to multifocal mammary tumor formation and drives activation of Ras and PI3K/AKT signaling. The MMTV-*PyMT* murine mammary tumor model exhibits characteristics of the ER^+ luminal subtype of human breast cancer, associated with four identifiable stages of tumor progression (hyperplasia, adenoma, early carcinoma, and late carcinoma) analogous to human breast tumors, followed by high frequency of metastasis to the lung (Lin et al., 2003). MMTV-*PyMT* male mice were mated with female *Pipp^{+/−}* mice to generate *PyMT;Pipp^{+/+}* and *PyMT;Pipp^{−/−}* mice (Figure 3A). Hyperplasia was detected in the mammary gland of control animals at 45 days and, notably, the number of hyperplastic foci in mammary fat pads of *PyMT;Pipp^{−/−}* mice was increased ∼5-fold (Figures 3B and 3C). In addition, the area of hyperplasia was increased at 45 (3-fold) and 70 (2.4-fold) days in *PyMT;Pipp^{−/−}*

mammary glands (Figures 3B and 3D), suggesting that *Pipp* ablation promotes breast cancer initiation. *Pipp* ablation significantly increased cell proliferation in PyMT-induced hyperplastic lesions (Figures 3E and 3F), associated with a significant increase in pAKT and pGSK3β staining intensity in the hyperplastic foci (Figures 3G and 3H).

To assess the effect of *Pipp* ablation on mammary cancer progression, tumor growth in *PyMT;Pipp^{+/+}* and *PyMT;Pipp^{−/−}* mice was measured twice weekly after tumor onset. The change in volume of the largest tumor in each mouse and the total tumor burden was significantly increased in *PyMT;Pipp^{−/−}* relative to *PyMT;Pipp^{+/+}* breast tumors (Figure 4A) and was associated with increased cell proliferation as shown by Ki67 staining (Figure 4B). In advanced tumors, the highest pAKT and pGSK3β staining was observed in tumor cells near the interface with surrounding mammary tissue in both *PyMT;Pipp^{+/+}* and *PyMT;Pipp^{−/−}* mice, but was more intense in *PyMT;Pipp^{−/−}* tumors (Figures 4C and 4D).

AKT activation is facilitated by PtdIns(3,4,5)P_3, which is dephosphorylated by PIPP to generate PtdIns(3,4)P_2. Both PtdIns(3,4,5)P_3 and PtdIns(3,4)P_2 are required for full AKT activation, however, the depletion of other PtdIns(3,4,5)P_3 5-phosphatases, such as SHIP1, SHIP2, INPP5E, and SKIP leads to enhanced AKT activation, suggesting increased levels of PtdIns(3,4,5)P_3 alone may be sufficient to activate AKT (Dyson et al., 2012; Ooms et al., 2009). The effect of *Pipp* ablation on plasma membrane phosphoinositide signals was assessed by immunofluorescence microscopy using PtdIns(3,4,5)P_3 and PtdIns(3,4)P_2 antibodies and phosphoinositide-specific biosensors. Plasma membrane PtdIns(3,4,5)P_3 signals were increased (1.2-fold) following growth factor stimulation in cell lines established from *PyMT;Pipp^{−/−}* primary tumors and MDA-MB-231 PIPP shRNA knockdown cells compared to controls (Figures S3A and S3B). In addition, increased plasma membrane recruitment (1.26-fold) of the PtdIns(3,4,5)P_3 biosensor GFP-PH/Btk was observed in *PyMT;Pipp^{−/−}* tumor cells following insulin-like growth factor 1 (IGF-I) stimulation (Figure S3C). Conversely, plasma membrane PtdIns(3,4)P_2 signals were decreased following growth factor stimulation in *PyMT;Pipp^{−/−}* tumor cells (1.18-fold) and MDA-MB-231 PIPP shRNA knockdown cells (1.38-fold) relative to controls at the same time point (Figures S3D and S3E). Furthermore, *Pipp* ablation impaired the plasma membrane recruitment of the PtdIns(3,4)P_2 biosensor YFP-PH/TAPP1 in response to IGF-I stimulation (Figure S3F).

In control studies, immunohistochemistry (IHC) staining of tumor sections revealed expression of the PyMT oncoprotein was similar in *PyMT;Pipp^{−/−}* and *PyMT;Pipp^{+/+}* mammary glands (Figure 4E). Therefore *Pipp* ablation in MMTV-*PyMT* mice significantly enhances primary mammary cancer initiation and tumor progression.

PIPP Regulates Cancer Cell Migration and Metastasis

Despite recent advances in breast cancer therapy, metastasis remains the leading cause of breast cancer death (Dumont et al., 2012). The MMTV-*PyMT* mouse model develops lung metastases at high frequency (Guy et al., 1992). To determine the influence of *Pipp* expression on metastasis, *PyMT;Pipp^{+/+}* and *PyMT;Pipp^{−/−}* lung tissue sections were examined for the presence of lung metastases. All mice developed lung metastases,
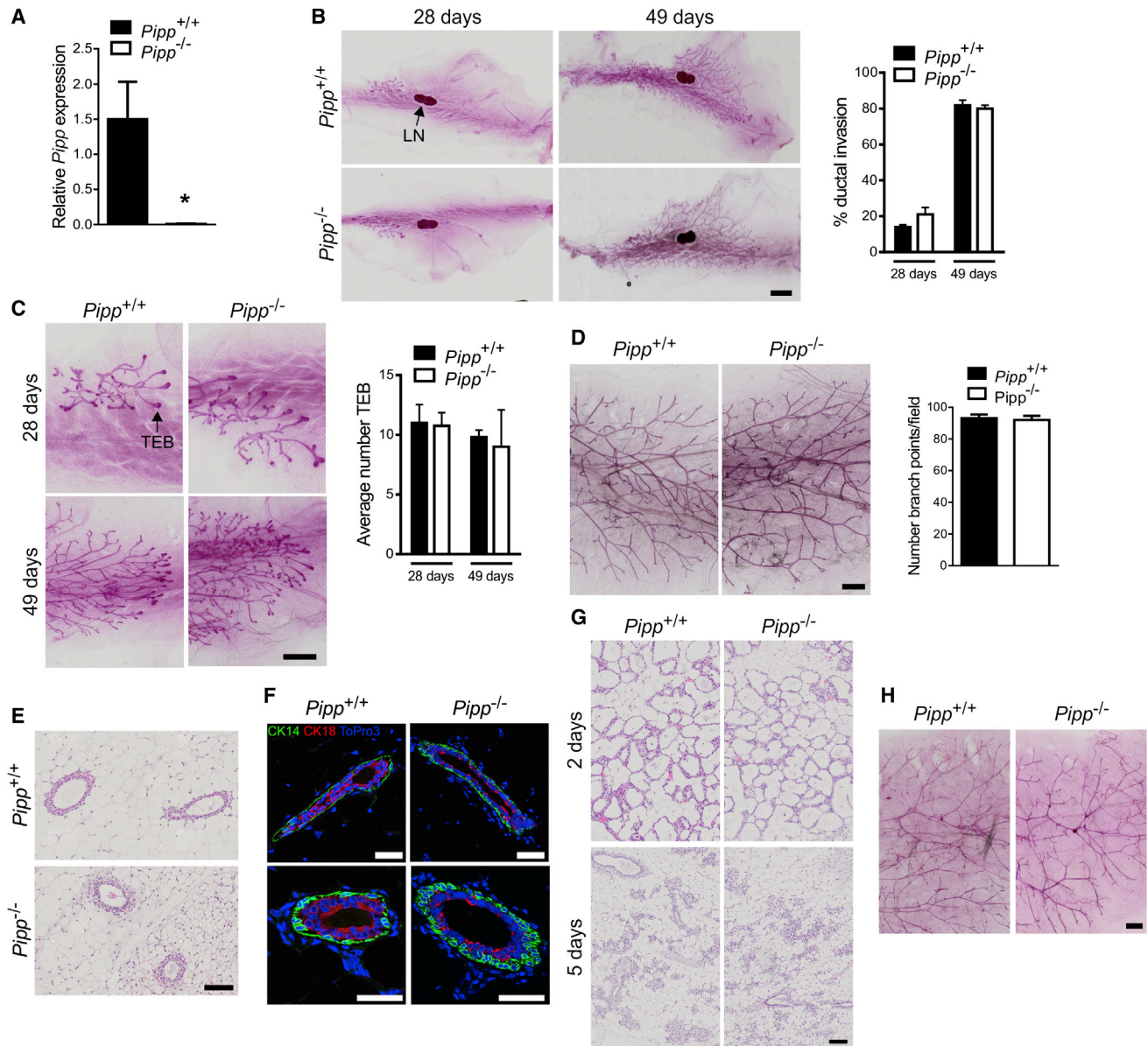
Figure 2. *Pipp*⁻/⁻ Mice Exhibit Normal Mammary Development

(A) *Pipp* exon 2 expression was quantified by quantitative (q)RT-PCR relative to glyceraldehyde 3-phosphate dehydrogenase (GAPDH) in mRNA extracted from brains of *Pipp*⁺/⁺ versus *Pipp*⁻/⁻ mice. The data represent mean *Pipp* expression ± SEM, n = 3 mice/genotype (*p < 0.05).

(B) Carmine alum stained mammary gland whole mounts from virgin *Pipp*⁺/⁺ and *Pipp*⁻/⁻ mice at 28 and 49 days of age. The data represent the mean percentage invasion of the epithelial tree into the mammary fat pad ± SEM from 28 (*Pipp*⁺/⁺ n = 3 and *Pipp*⁻/⁻ n = 4) and 49 day (*Pipp*⁺/⁺ n = 5 and *Pipp*⁻/⁻ n = 7) mice (lymph node, LN).

(C) Magnified images of Carmine alum stained mammary gland whole mounts from 28- and 49-day-old *Pipp*⁺/⁺ and *Pipp*⁻/⁻ mice showing terminal end buds (TEB). The data represent the mean number of TEB/gland ± SEM from 28- (*Pipp*⁺/⁺ n = 3 and *Pipp*⁻/⁻ n = 4) and 49-day-old (*Pipp*⁺/⁺ n = 5 and *Pipp*⁻/⁻ n = 7) mice.

(D) Mammary gland whole mounts were prepared as above from 16-week-old *Pipp*⁺/⁺ and *Pipp*⁻/⁻ mice. The data represent the mean number of branch points ± SEM from *Pipp*⁺/⁺ (n = 12) and *Pipp*⁻/⁻ (n = 11) mice.

(E and F) Formalin fixed, paraffin embedded (FFPE) sections of fourth mammary glands from 16-week-old *Pipp*⁺/⁺ and *Pipp*⁻/⁻ mice were stained with hematoxylin and eosin (H&E) (E) or immunostained with CK14 (green) and CK18 (red) antibodies and counterstained with To-Pro-3 to detect nuclei (blue) (F).

(G) Hematoxylin and eosin (H&E) stained, formalin fixed, paraffin embedded (FFPE) mammary gland sections from *Pipp*⁺/⁺ and *Pipp*⁻/⁻ mice at 2 and 5 days involution.

(H) Carmine alum stained mammary gland whole mounts from 1-year-old *Pipp*⁺/⁺ and *Pipp*⁻/⁻ mice. The scale bars represent 2 mm (B), 1 mm (C, D, and H), 100 μm (E and G), and 50 μm (F). See also Figure S2.
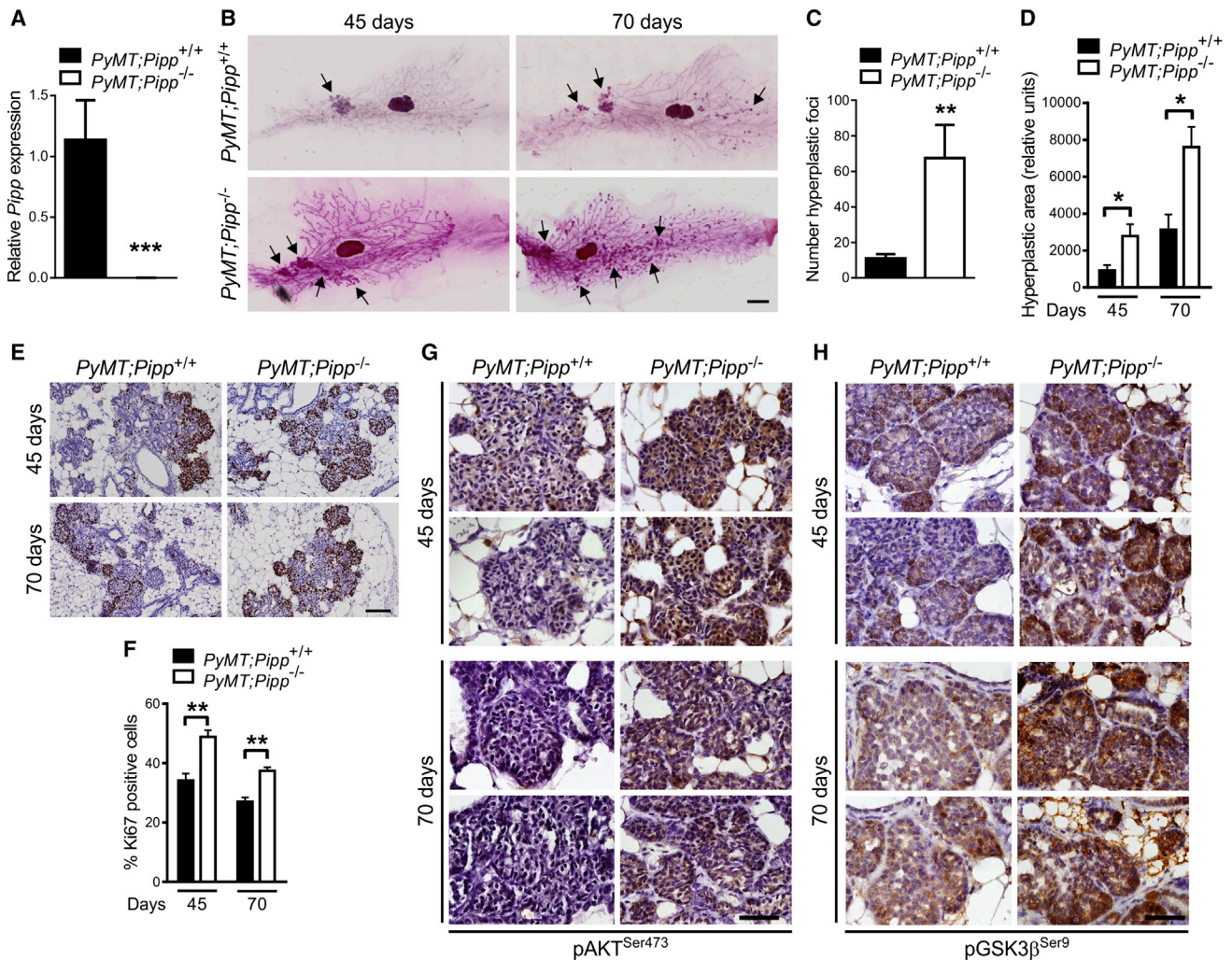
Figure 3. *Pipp* Ablation Promotes Tumor Initiation in PyMT Model Mice

(A) *Pipp* exon 2 expression was quantified by qRT-PCR relative to GAPDH in mRNA extracted from mammary tumors of *PyMT;Pipp*^{+/+} versus *PyMT;Pipp*^{−/−} mice. The data represent mean *Pipp* expression ± SEM, n = 7 mice/genotype.

(B–D) *Pipp* ablation is associated with increased numbers and size of hyperplastic foci (arrows) in the mammary glands of 45- and 70-day-old *PyMT* mice (B). The data represent the mean number of hyperplastic foci per mammary gland ± SEM from 45-day-old *PyMT;Pipp*^{+/+} (n = 6) and *PyMT;Pipp*^{−/−} (n = 6) mice (C). The total area of hyperplastic foci in mammary gland whole mounts was measured using ImageJ. The data represent the mean area of hyperplasia ± SEM from 45- (n = 6 mice/genotype) and 70-day-old (*PyMT;Pipp*^{+/+} n = 8 and *PyMT;Pipp*^{−/−} n = 9) mice (D).

(E and F) Ki67 immunostaining of mammary gland sections from 45- and 70-day-old *PyMT;Pipp*^{+/+} and *PyMT;Pipp*^{−/−} mice (E). The data represent the mean percentage of Ki67 positive cells ± SEM in the hyperplastic lesions of 45 (*PyMT;Pipp*^{+/+} n = 6 and *PyMT;Pipp*^{−/−} n = 5) and 70-day-old (*PyMT;Pipp*^{+/+} n = 8 and *PyMT;Pipp*^{−/−} n = 9) mice (F).

(G and H) Representative images of pAKT[Ser473] (G) and pGSK3β[Ser9] (H) immunostaining of mammary gland sections from 45- and 70-day-old *PyMT;Pipp*^{+/+} and *PyMT;Pipp*^{−/−} mice. The scale bars represent 2 mm (B) and 100 μm (E, G, and H) (*p < 0.05, **p < 0.01, and ***p < 0.001).

irrespective of *Pipp* status. Interestingly however, the total number of lung metastases was significantly lower in *PyMT;Pipp*^{−/−} compared to *PyMT;Pipp*^{+/+} mice (4.3-fold decrease) (Figures 5A and 5B). Therefore, loss of *Pipp* impairs breast cancer metastasis despite promoting increased primary tumor growth.

As *Pipp* ablation impaired mammary cancer metastasis in vivo, we next examined whether loss of *PIPP* affected breast cancer cell growth and invasion using organotypic assays. Control and *PIPP* shRNA knockdown MDA-MB-231 cells were seeded onto organotypic matrices consisting of human fibroblast-contracted rat tail collagen and cultured for 10 or 14 days.

PIPP depletion did not affect the fraction of cells in the upper section of the matrix (0–100 μm), but significantly reduced the percentage of invading cells at both 10 and 14 days (Figures 5C and 5D). In addition, *PIPP* shRNA expressing MDA-MB-231 cells above the matrix exhibited increased cell proliferation after 10 days, but no change in the number of apoptotic cells (Figures 5E, 5F, and S4). These results suggest that *PIPP* depletion promotes breast cancer cell proliferation, but impairs invasion, consistent with the increased primary tumor growth, but decreased metastasis observed in *PyMT;Pipp*^{−/−} mice.
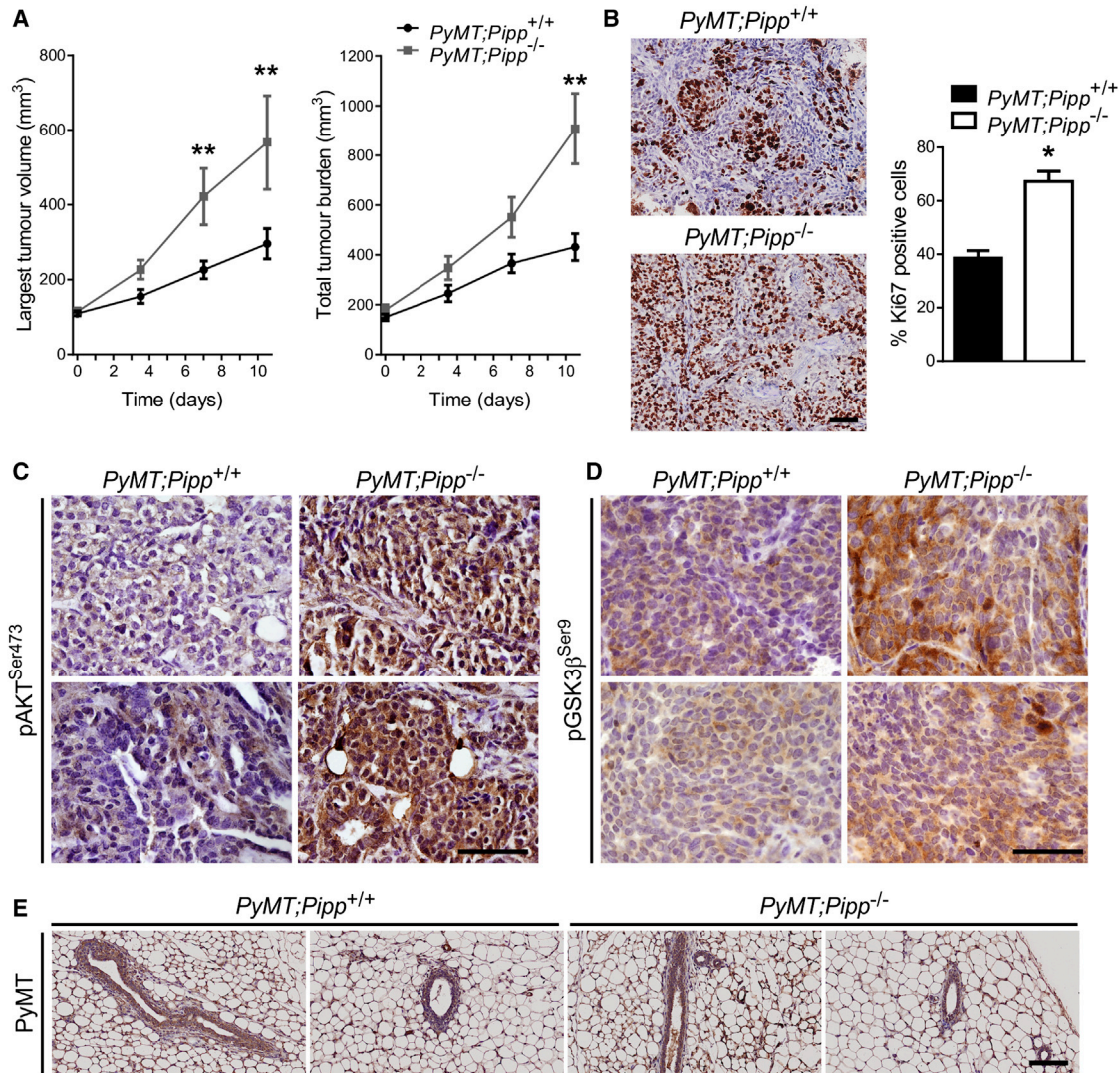
Figure 4. *Pipp* Ablation Promotes Tumor Growth in PyMT Model Mice

(A) Graphs show the mean volume ± SEM of the largest tumor per mouse and total tumor volume (mm³) after diagnosis (time 0) from *PyMT;Pipp*^{+/+} (n = 12) and *PyMT;Pipp*^{−/−} (n = 10) mice. The largest tumor in all mice exhibited the same size (∼100 mm³) at diagnosis (time 0).

(B) Ki67 staining of mammary tumor sections. The data represent the mean percentage of Ki67 positive cells ± SEM in tumors from seven mice/genotype.

(C and D) Representative images of tumor sections from *PyMT;Pipp*^{+/+} and *PyMT;Pipp*^{−/−} mice stained with antibodies specific for pAKT^{Ser473} (C) or pGSK3β^{Ser9} (D).

(E) Representative images of mammary gland sections from *PyMT;Pipp*^{+/+} and *PyMT;Pipp*^{−/−} mice stained with an antibody specific for PyMT. The scale bars represent 100 μm (B and E) and 50 μm (C and D) (*p < 0.05 and **p < 0.01). See also Figure S3.

AKT is a major effector of oncogenic PI3K signaling in cancer. There are three AKT isoforms, AKT1, AKT2, and AKT3, that have been identified, each with non-redundant functions in breast cancer. A hotspot mutation, E17K, occurs in *AKT1* in ∼3%–8% of breast cancers (Carpten et al., 2007; Kim et al., 2008) and AKT3 is upregulated in triple negative breast cancers (Chin et al., 2014a). In breast cancer, particularly in the context of metastasis, there is emerging evidence that AKT1 and AKT2 play distinct functional roles. For example, expression of constitutively active AKT1 in murine mammary tissue does not drive de novo mammary tumor formation (Dillon et al., 2009; Hutchinson et al., 2004). However, in transgenic oncogene-driven murine

models of breast cancer, AKT1 induces primary tumor growth, but inhibits metastasis in vivo (Dillon et al., 2009; Hutchinson et al., 2004). In contrast, the results from analysis of *Akt1* knockout mice are conflicting, with one study demonstrating reduced lung metastases and another increased metastases in MMTV-*neu* mice (Ju et al., 2007; Maroulakou et al., 2007). On the other hand, expression of constitutively active AKT2 promotes metastasis in murine breast cancer models (Dillon et al., 2009). To determine whether the reduction in metastasis observed in *PyMT;Pipp*^{−/−} mice was associated with impaired cancer cell migration, we evaluated cell migration in scratch wound healing assays using MDA-MB-231 control and *PIPP*
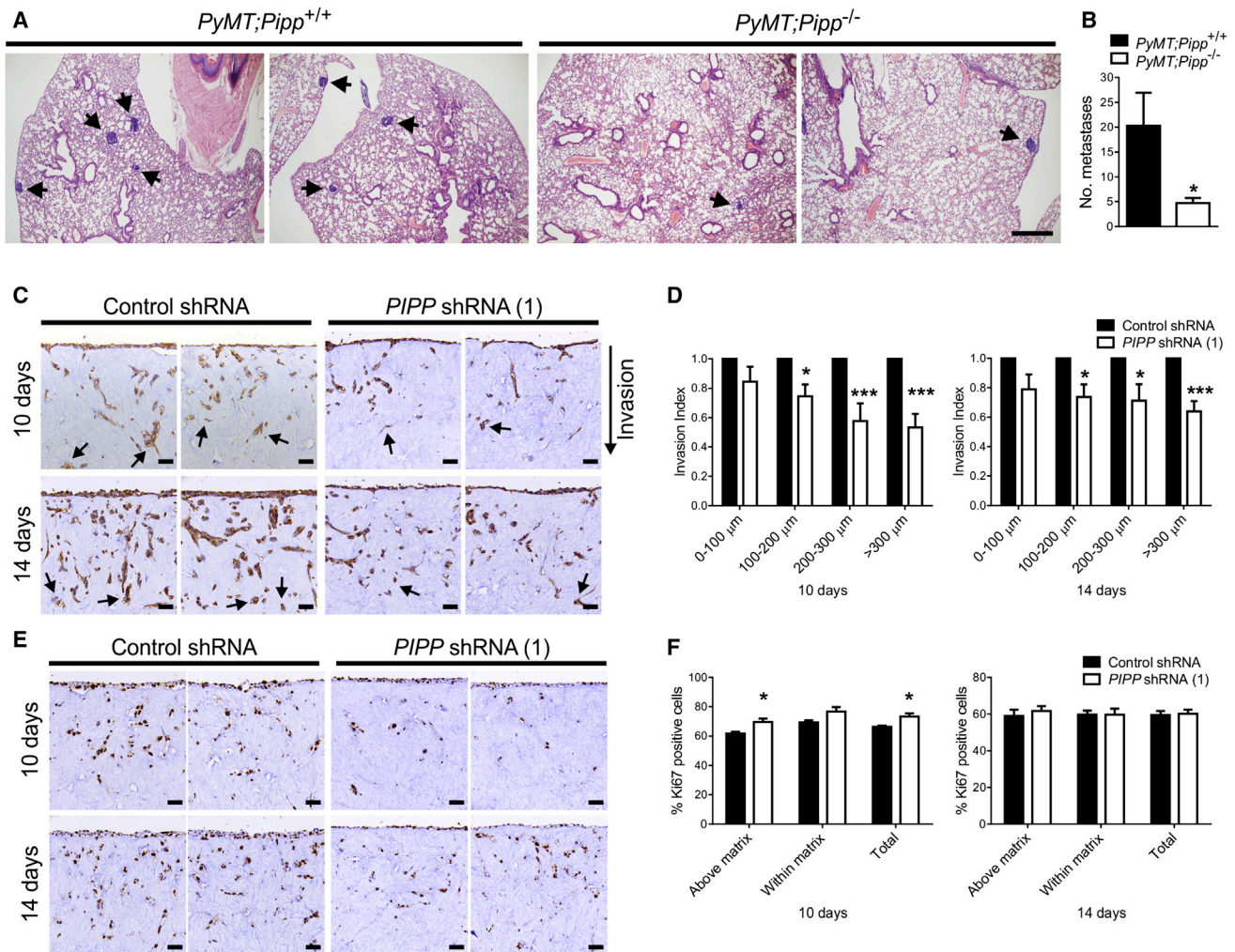
Figure 5. *Pipp* Depletion Impairs Breast Cancer Metastasis and Cell Invasion

(A and B) Formalin fixed, paraffin embedded (FFPE) lung sections from *PyMT;Pipp*$^{+/+}$ and *PyMT;Pipp*$^{-/-}$ mice were stained with hematoxylin and eosin (H&E) to identify metastases (arrows) (A). The data represent the mean total number of metastases from five lung sections/mouse ± SEM from *PyMT;Pipp*$^{+/+}$ (n = 11) and *PyMT;Pipp*$^{-/-}$ (n = 10) mice (B).

(C and D) Control shRNA or *PIPP* shRNA (1) expressing MDA-MB-231 cells were seeded onto organotypic matrices, cultured for 10 or 14 days, and stained for multi-cytokeratin (C), arrows indicate invading cells. The average number of invasive cells at 0–100 μm, 100–200 μm, 200–300 μm, and >300 μm were counted in ten representative images and normalized to the number of cells on top of the organotypic matrix. The results are expressed relative to control shRNA expressing cells at each depth, which were arbitrarily assigned a value of one. The data represent mean ± SEM, n = 5 (D).

(E and F) Representative images of organotypic matrices seeded with MDA-MB-231 cells and stained for Ki67 (E). The percentage of proliferating cells on top or within the matrix was quantified in ten representative images normalized to the total number of cells present after 10 or 14 days invasion. The data represent mean ± SEM, n = 5 (F). The scale bars represent 500 μm (A) and 50 μm (C and E) (*p < 0.05 and ***p < 0.001). See also Figure S4.

shRNA knockdown cells. *PIPP* shRNA knockdown significantly reduced wound healing with ~50%–60% wound closure after 36 hr compared to ~90% closure in controls (Figures 6A and 6B). Individual cell tracking revealed control cells migrated in a directed manner into the wound. In contrast, *PIPP* shRNA knockdown cells exhibited random migration and cells traveled perpendicular to, rather than migrating into, the wound (Figure 6C). *PIPP* depletion also impaired cell migration toward a chemoattractant (3.2-fold decrease), a phenotype partially rescued by treatment with the pan-AKT inhibitor, AktX (Figures 6D and 6E). To confirm these observations, cell lines were established from *PyMT;Pipp*$^{-/-}$ and *PyMT;Pipp*$^{+/+}$ primary mammary

tumors. *PyMT;Pipp*$^{-/-}$ tumor cells exhibited a 3.5-fold decrease in migration toward a chemoattractant (Figures 6F, 6G, and S5) that was in part rescued by treatment with AktX (Figures 6F and 6G). These results suggest that the cell migration defect observed in *PIPP*-deficient cells is a consequence of dysregulated AKT signaling.

PIPP Regulates NFAT1, TSC2, and *Mmp2* Expression

As AKT1 and AKT2 play opposing roles in regulating cell migration and metastasis, we next examined whether the cell migration defect in *PIPP*-deficient cells was AKT isoform-dependent. Droplet digital PCR analysis revealed *Akt1* as the predominant
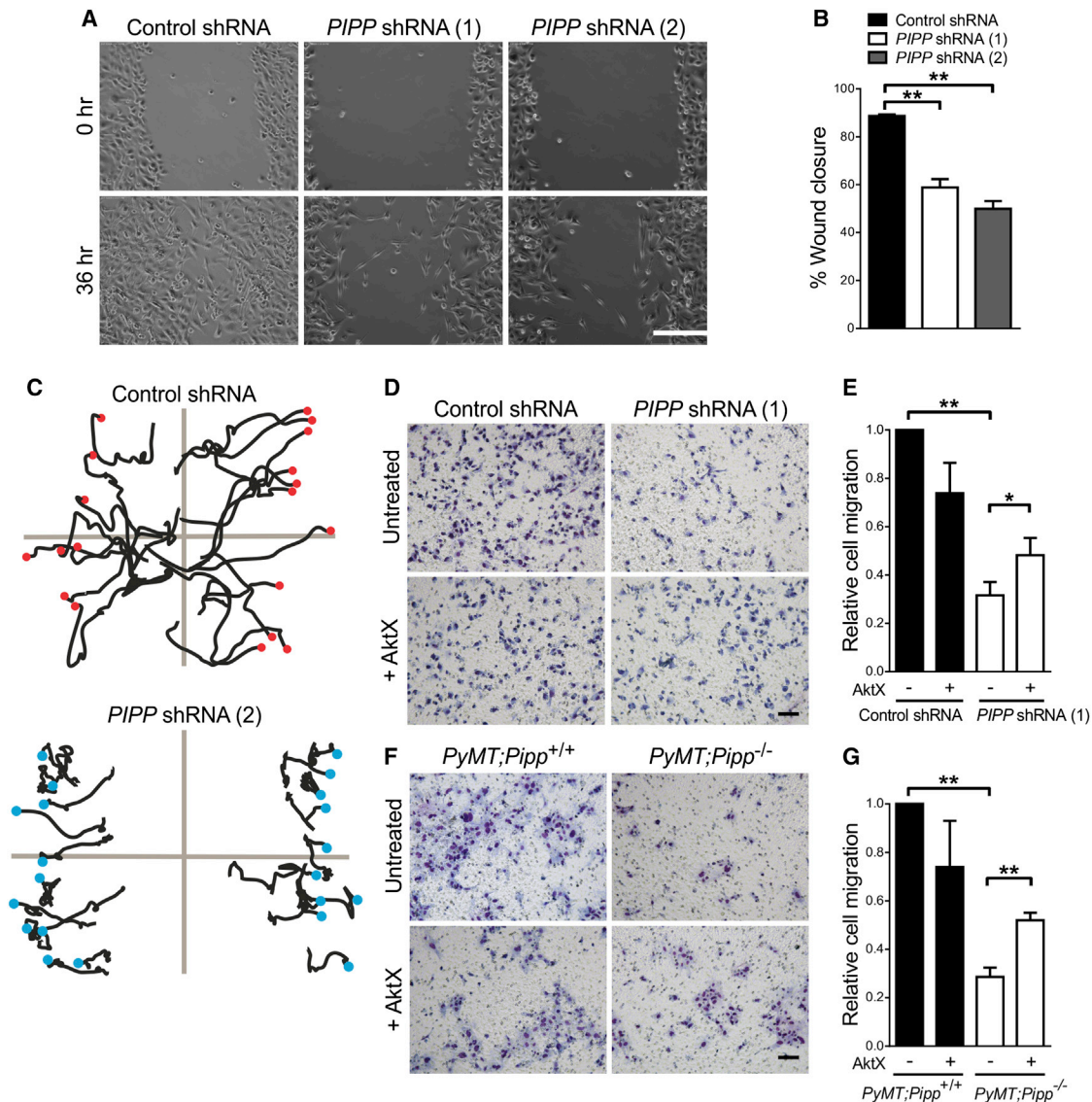
Figure 6. *PIPP* Depletion Impairs Breast Cancer Cell Migration

(A–C) Confluent monolayers of MDA-MB-231 cells expressing control or *PIPP* shRNA (1) or (2) were wounded, and cell migration into the wound monitored by live cell microscopy. The representative images show the same area at 0 hr and after 36 hr incubation (A). The data represent mean percentage wound closure ± SEM, n = 3 (B). The migration of individual cells over 36 hr was tracked using ImageJ (C) (n ≥ 20 cells/sample, representative of three experiments).

(D and E) Migration of control and *PIPP* shRNA (1) expressing MDA-MB-231 cells toward a serum gradient was measured using Transwell assays ± a pan-AKT inhibitor, AktX (D). The results are expressed relative to untreated control shRNA expressing cells. The data represent mean ± SEM, n = 4 (E).

(F and G) Epithelial tumor cell lines were established from mammary tumors from *PyMT;Pipp*^{+/+} and *PyMT;Pipp*^{−/−} mice. The cell migration toward a serum gradient was determined using Transwell assays ± AktX (F). The results are expressed relative to untreated *PyMT;Pipp*^{+/+} cells. The data represent mean ± SEM, n = 3 (G). The scale bars represent 250 μm (A) and 100 μm (D and F) (*p < 0.05 and **p < 0.01). See also Figure S5.

isoform expressed in *PyMT;Pipp* mammary tumor epithelial cell lines (Figure 7A). MDA-MB-231 cells exhibited similar levels of *AKT1* and *AKT2* expression (Figure S6A). *AKT* isoform expression was not affected by *PIPP* depletion in either *PyMT;Pipp* mammary tumor epithelial or MDA-MB-231 cells (Figures 7A and S6A). To assess whether PIPP depletion results in differential AKT isoform activation, MDA-MB-231 shRNA cells were immunoblotted with pAKT1 versus pAKT2-specific antibodies as described (Chew et al., 2015; Chin et al., 2014b). Phosphorylation of both AKT1 and AKT2 was increased in MDA-MB-231

PIPP shRNA cells in response to EGF stimulation (Figure S1F), suggesting PIPP inhibition of AKT activation is not isoform specific.

To determine whether AKT1 or AKT2 was responsible for the observed cell migration defect in *PIPP*-deficient cells, shRNA-mediated knock down of *Akt1* or *Akt2* was undertaken in *PyMT:Pipp* mammary tumor cell lines resulting in 73%–89% and 67%–91% knock down, respectively (Figures S6B–S6D). Notably, *PyMT;Pipp*^{−/−} cell migration was restored to wild-type levels by shRNA knock down of *Akt1*, but not *Akt2* (Figures 7B and 7C).
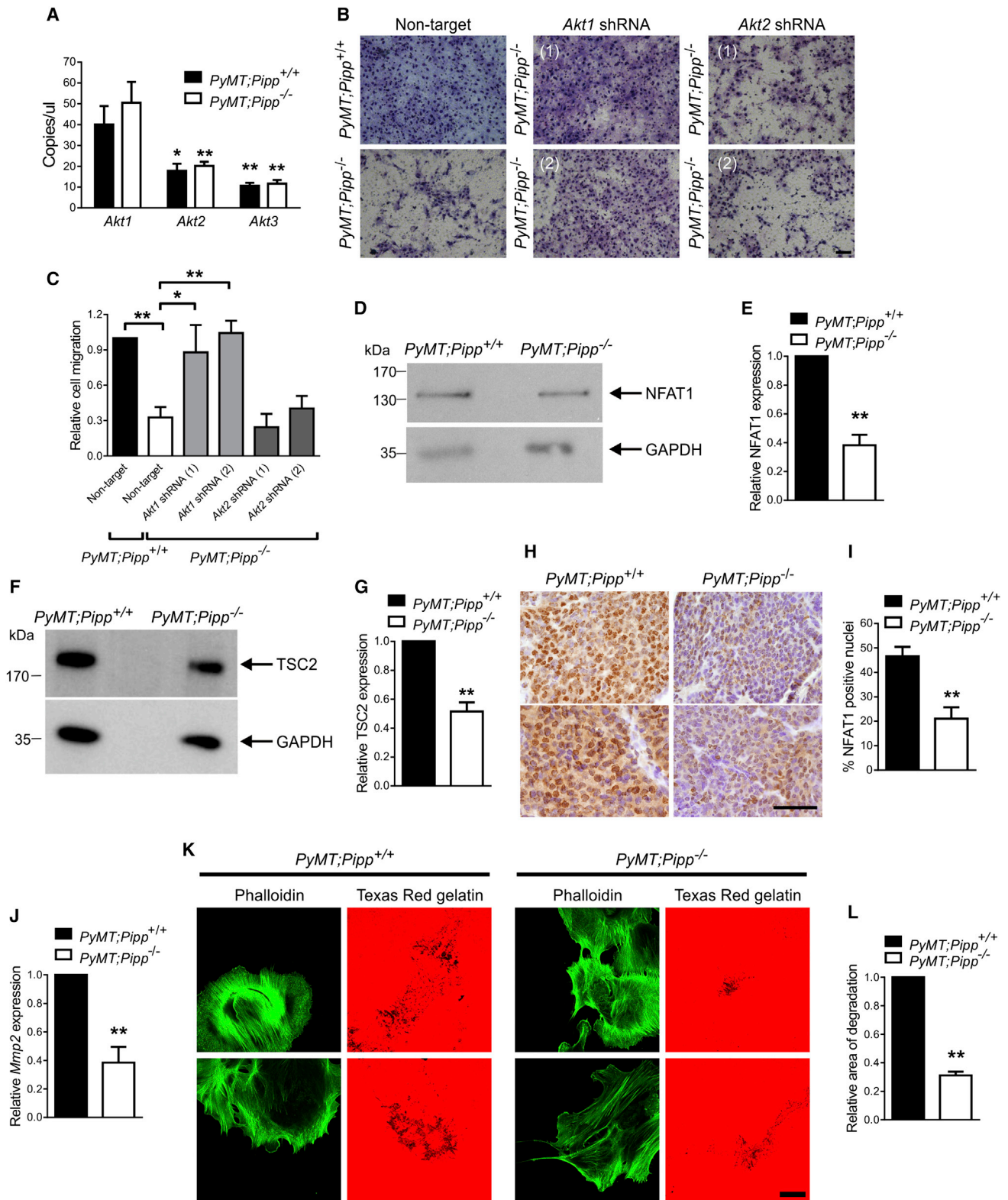
Figure 7. *Pipp* Knockout Impairs AKT1-Mediated Migration in *PyMT;Pipp* Tumor Cells

(A) Absolute *Akt1*, *Akt2*, and *Akt3* expression was quantified by droplet digital PCR in mRNA extracted from *PyMT;Pipp*^{+/+} versus *PyMT;Pipp*^{−/−} mammary epithelial tumor cell lines. The data represent mean *Akt* isoform expression ± SEM, n = 3.

(legend continued on next page)

AKT1 inhibits the migration of breast cancer cells, and thereby invasion and metastasis, by regulating the protein levels or activity of several effectors (Chin and Toker, 2009). AKT1 phosphorylates and, thereby, destabilizes the tumor suppressor tuberous sclerosis complex 2 (TSC2), a Rho-GTPase regulator that influences cell migration via regulation of F-actin assembly (Astrinidis et al., 2002). AKT1 also phosphorylates and regulates the protein levels of NFAT1, a pro-invasion transcription factor (Yoeli-Lerner et al., 2005, 2009). Furthermore, AKT1 phosphorylates palladin and promotes its actin-bundling function (Toker, 2012). To assess the effects of loss of *PIPP* on AKT1 downstream effectors, *PyMT;Pipp*$^{-/-}$ tumor and MDA-MB-231 *PIPP* shRNA cell lines were analyzed for NFAT1 and TSC2 protein expression by immunoblot analysis, revealing decreased protein levels (Figures 7D–7G and S6E–S6J). *PyMT;Pipp*$^{-/-}$ tumors also exhibited significantly decreased NFAT1 positive nuclei compared to *PymT;Pipp*$^{+/+}$ tumors (Figures 7H and 7I).

Cancer cells invade through the extracellular matrix by degrading collagen type IV, a major structural component of the basement membrane. Matrix metalloproteinase 2 (MMP2) digests a number of substrates including collagen type IV and gelatin and plays a role in breast cancer cell invasion and metastasis (Chabottaux and Noel, 2007; Jezierska and Motyl, 2009). AKT1 regulates MMP2 expression in cultured breast cancer cells (Park et al., 2001). *PyMT;Pipp*$^{-/-}$ tumor-derived and MDA-MB-231 *PIPP* shRNA cell lines exhibited reduced *Mmp2* expression relative to control cells (Figures 7J, S6K, and S6L). Consistent with these observations, *PyMT;Pipp*$^{-/-}$ tumor and MDA-MB-231 *PIPP* shRNA cell lines showed reduced matrix degradation (Figures 7K, 7L, S6M, and S6N). Therefore, we conclude that loss of *PIPP* impairs breast cancer cell migration and matrix degradation through increased AKT1 activity and, thereby, decreased NFAT1, TSC2, and *Mmp2* expression.

PIPP and *AKT1* mRNA Expression Is Decreased in ER$^-$ Human Primary Breast Cancers

PIPP mRNA expression is decreased in ER$^-$ versus ER$^+$ breast tumors (Gruvberger et al., 2001; van 't Veer et al., 2002), but *PIPP* expression has not been correlated with breast cancer subtype. Here, *PIPP* mRNA expression was evaluated using TissueScan Breast Cancer cDNA Arrays I–IV (OriGene) of 16 normal breast tissues and 176 primary human breast cancer samples. *PIPP* mRNA

expression was reduced in ER$^-$ breast tumors relative to ER+ tumors (Figure 8A). Luminal breast cancers express ER and/or PR and in general have good outcomes, relative to triple negative cancers (ER$^-$/PR$^-$/HER2$^-$), which exhibit poor prognosis (Voduc et al., 2010). *PIPP* mRNA expression was significantly decreased in triple negative breast cancers, relative to normal breast tissue or luminal breast cancers (Figure 8B).

As *PIPP* depletion was identified here to inhibit AKT1-dependent cell migration, we evaluated *AKT1* expression in the same breast cancer cohort. *AKT1* expression also showed a positive correlation with ER status (Figure 8A) and was significantly lower in triple negative tumors relative to normal breast tissue or luminal breast cancers (Figure 8B). Therefore, *PIPP* exhibits a similar pattern of mRNA expression to *AKT1* in human breast cancers. To further explore the association between *PIPP* and *AKT1*, we examined tumors with a >2-fold reduction in *PIPP* and *AKT1* expression relative to normal breast tissue. There were 85% of ER$^+$ breast cancers that showed *PIPP/AKT1* expression comparable to normal breast tissue levels, whereas 71% of ER$^-$ tumors exhibited low *PIPP/AKT1* mRNA expression (p < 0.001; Figure 8C), suggesting that expression of both *PIPP* and *AKT1* is reduced in ER$^-$ breast cancers. Examination of the Kaplan-Meier-Plotter data set (Györffy et al., 2010) revealed that lower *PIPP* expression predicted for reduced relapse-free and overall survival (Figures 8D and 8E).

DISCUSSION

Mutation of *PIK3CA* is one of the most common events in ER$^+$ breast cancer (Ma and Ellis, 2013; Pang et al., 2014). Here, we identify the inositol polyphosphate 5-phosphatase PIPP as a suppressor of oncogenic PI3K/AKT signaling in breast cancer. *PIPP* shRNA knockdown increased breast cancer cell proliferation, reduced apoptosis, increased anchorage independent cell growth, and enhanced xenograft tumor growth, associated with increased AKT signaling. PIPP also suppressed oncogenic PI3K/AKT signaling in vivo. *Pipp* knockout in an oncogene-driven murine breast cancer model increased primary breast tumor growth, and the tumors showed increased AKT signaling. In human breast tumors, *PIPP* expression was reduced in triple negative breast cancers and was associated with reduced long-term survival.

(B and C) Migration of *PyMT;Pipp*$^{+/+}$ cells stably expressing non-target shRNA or *PyMT;Pipp*$^{-/-}$ cells stably expressing non-target *Akt1* (1) or (2) or *Akt2* (1) or (2) shRNAs toward a serum gradient was determined using Transwell assays (B). The results are expressed relative to untreated *PyMT;Pipp*$^{+/+}$ cells expressing non-target shRNA. The data represent mean ± SEM, n = 4 (C).

(D) Lysates of mammary tumor cell lines from *PyMT;Pipp*$^{+/+}$ and *PyMT;Pipp*$^{-/-}$ mice were immunoblotted with antibodies specific for NFAT1 or GAPDH as a loading control.

(E) Densitometric analysis of NFAT1 expression normalized to GAPDH. The results are expressed relative to *PyMT;Pipp*$^{+/+}$ tumor cells, which were arbitrarily assigned a value of one. The data represent mean ± SEM, n = 3.

(F) Lysates of mammary tumor cell lines from *PyMT;Pipp*$^{+/+}$ and *PyMT;Pipp*$^{-/-}$ mice were immunoblotted with antibodies specific for TSC2 or GAPDH as a loading control.

(G) Densitometric analysis of TSC2 expression normalized to GAPDH. The results are expressed relative to *PyMT;Pipp*$^{+/+}$ tumor cells, which were arbitrarily assigned a value of one. The data represent mean ± SEM, n = 5.

(H and I) Representative images of tumor sections from *PyMT;Pipp*$^{+/+}$ and *PyMT;Pipp*$^{-/-}$ mice stained with antibodies specific for NFAT1 (H). The data represent the mean percentage of cells exhibiting NFAT1 positive nuclei ± SEM in tumors from seven mice/genotype (I).

(J) *Mmp2* expression was quantified by qRT-PCR relative to GAPDH in mRNA extracted from *PyMT;Pipp*$^{+/+}$ versus *PyMT;Pipp*$^{-/-}$ mammary tumor cell lines. The data represent mean *Mmp2* expression ± SEM in tumor cell lines, n = 3.

(K and L) *PyMT;Pipp* tumor cells were plated on Texas red-labeled gelatin (red) coated coverslips for 48 hr then fixed and stained with Alexa 488-phalloidin (green) to label F-actin (K). The regions of matrix degradation appear as dark spots in the Texas red gelatin images. The data represent mean area of degraded matrix ± SEM, n = 3 (L). The scale bars represent 100 μm (B), 50 μm (H), and 10 μm (K) (*p < 0.05 and **p < 0.01). See also Figure S6.
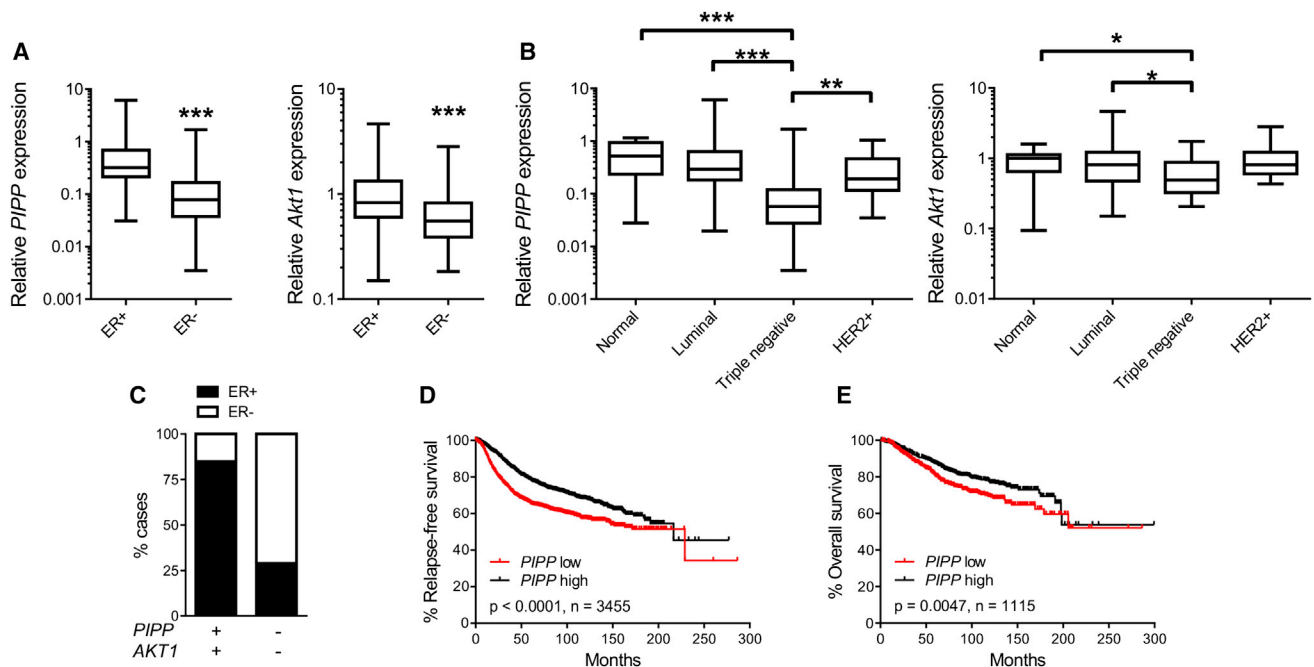
Figure 8. PIPP and AKT1 mRNA Expression Is Decreased in ER⁻ Primary Human Breast Cancers

(A and B) Normalized *PIPP* and *AKT1* mRNA expression was determined by qRT-PCR using TissueScan Breast Cancer Arrays I-IV with *PIPP*, *AKT1*, and β-actin primers. The data are displayed as box and whiskers on a log scale. The *PIPP* and *AKT1* expression was correlated with (A) ER (140 cases) or (B) breast cancer subtype (135 cases). p values were determined using a two-tailed Mann-Whitney test (*p < 0.05, **p < 0.01, and ***p < 0.001).

(C) Breast cancer cases were scored for normal (*PIPP⁺/AKT1⁺*) versus low (*PIPP⁻/AKT1⁻*) *PIPP* and *AKT1* mRNA expression in ER⁺ and ER⁻ tumors (75 cases). The significance was determined using a Fisher's exact test (p < 0.001).

(D and E) Correlation of *PIPP* mRNA levels with breast cancer survival. Kaplan-Meier plots of relapse-free (D) and overall (E) patient survival stratified by median *PIPP* expression in the KM Plotter breast cancer meta-analysis database (Györffy et al., 2010). The statistical significance was determined using a log rank test.

This study has identified a breast tumor regulatory role for an inositol polyphosphate 5-phosphatase. Although many of the ten mammalian 5-phosphatases hydrolyze PtdIns(3,4,5)P₃ and suppress AKT signaling in cultured cells, a tumor suppressive role for this enzyme family analogous to PTEN is slow to emerge. The hematopoietic-specific *SHIP1* is mutated in rare cases of acute myeloid leukemia, associated with amplified PI3K/AKT signaling and *Ship1* knockout mice exhibit hematopoietic cell expansion (reviewed in Ooms et al., 2009). The 5-phosphatase SKIP suppresses PTEN-deficient U87MG cell proliferation, and its increased expression predicts for improved outcomes in glioblastoma (Davies et al., 2014). *PIPP* expression is reduced in human melanomas, and ectopic expression or shRNA knock down of *PIPP* in melanoma-derived cultured cell lines results in altered cell proliferation and transformation (Ye et al., 2013). Recently, PIPP was also identified as a target for micro-RNAs in squamous cell carcinoma (Lin et al., 2014). However, no murine knockout for *Pipp* has been reported and therefore its function as a tumor suppressor in vivo has not been tested. Here, *Pipp⁻/⁻* mice showed normal mammary gland development and did not develop mammary tumors. Notably, loss of *Pipp* in MMTV-*PyMT* mice resulted in increased mammary hyperplasia, with accelerated growth of hyperplastic foci and established tumors. Similarly, constitutively active AKT1 expression also promotes tumor cell proliferation and mammary tumor growth in MMTV-*neu* mice (Young et al., 2008), but transgenic expression of constitutively active AKT1 alone in the mammary gland does

not promote de novo tumor formation (Hutchinson et al., 2001; Schwertfeger et al., 2001). The effects of *Pipp* ablation on tumor development in MMTV-*PyMT* mice may be cell autonomous or stromal-dependent, as *Pipp* was deleted in all tissues, including the stroma. Xenograft studies using MDA-MB-231 cells with *PIPP* knockdown suggest a cell autonomous role for PIPP in suppressing mammary tumor development, however, further studies will be required to delineate the effects of PIPP expression in stromal versus epithelial mammary cells.

Surprisingly, although *Pipp* ablation significantly increased mammary tumor growth in MMTV-*PyMT* mice, this was associated with reduced lung metastases. However, it should be noted that although *PyMT;Pipp⁻/⁻* mice exhibited decreased numbers of metastases, loss of *Pipp* did not alter the percentage of mice that developed lung metastases. It is conceivable that loss of *PIPP* expression reduces the metastatic potential of human breast cancers, however, the increased proliferative advantage of any *PIPP*-deficient cells that do metastasize may facilitate establishment and growth of tumor foci at distant sites. AKT1 and AKT2 exhibit opposing effects on breast cancer cell migration, invasion, and metastasis (Arboleda et al., 2003; Chin and Toker, 2009; Yoeli-Lerner et al., 2005). Notably, AKT1 and AKT2 are activated to the same extent by growth factor stimulation and by the same upstream kinases and/or oncogenic PI3K. We have no evidence that PIPP inhibits the activation of specific AKT isoforms. Rather, as AKT1 is the dominant isoform in PyMT breast cancer cells, as reported previously (Maroulakou et al.,

2007), it is likely *PIPP* loss of expression results in greater activation of the total AKT1 pool over AKT2. In addition, it is not clear whether AKT1 exerts more significant effects on cell migration and invasion than the opposing actions mediated by AKT2, when both these kinases are co-expressed. Therefore, we propose in the experimental models used here, *PIPP* loss activates AKT, which in turn suppresses cell migration through several downstream effectors of AKT1 including TSC2 and NFAT1. AKT1 promotes the degradation of TSC2, resulting in decreased activation of Rho, and also regulates the stability and protein expression of the transcription factor NFAT (Astrinidis et al., 2002; Larkins et al., 2006; Yoeli-Lerner et al., 2005, 2009). Expression of myristoylated AKT1 decreases TSC2 levels in T4-2 breast cancer cells and tumor xenografts, resulting in cell migration and invasion defects that are rescued by exogenous TSC2 expression (Liu et al., 2006). AKT1 activation promotes degradation of the transcription factor NFAT1 in a GSK3β-dependent manner (Yoeli-Lerner et al., 2005, 2009). *PIPP*-deficient cells exhibited significantly impaired cell migration associated with reduced expression of AKT1-dependent effectors NFAT1 and TSC2. Consistent with these observations, pan-AKT inhibition and shRNA knock down of *Akt1*, but not *Akt2*, rescued the cell migration defect in *PIPP*-deficient cells. We propose a model whereby loss of *Pipp* expression in breast cancers promotes AKT activation, leading to increased mammary tumor growth, but impaired AKT1-dependent cell migration and metastasis.

Notably, *PIPP* is expressed in ER$^+$ human breast cancers, but its expression is reduced in the poor prognosis triple negative human breast cancer subtype. Low *PIPP* expression is associated with poor long-term outcome, which appears counterintuitive to our observation of reduced lung metastases in *PyMT;Pipp*$^{-/-}$ mice. However, this apparent paradox could be explained by differences in AKT isoform expression and/or activity in primary human breast cancers. The relative expression of AKT1 in human breast tumors is complex and may relate to the breast cancer subtype. In our study of human tumors, *AKT1* mRNA expression correlated with both ER status and *PIPP* expression and was significantly decreased in triple negative breast cancers. Several other studies, however, have reported no correlation between AKT1 mRNA or protein expression and ER status (Creighton, 2007; Grell et al., 2012; Stål et al., 2003), although pAKT1 levels were reported as higher in ER$^+$ than ER$^-$ tumors (Gershtein et al., 2007). In addition, increased AKT1 kinase activity has been reported in 45% of primary breast cancers (Sun et al., 2001). It is interesting to speculate breast cancers with decreased *PIPP* and *AKT1* expression may still express activated AKT2, which in turn promotes metastasis leading to poorer outcomes.

Breast cancer deaths are most frequently caused by metastatic disease rather than the primary tumor, therefore, understanding the molecular mechanisms that regulate metastasis are critically important. Identifying biomarkers of metastasis may facilitate the development of effective tailored therapies to improve patient outcomes. Collectively, our studies suggest analysis of *PIPP* expression in breast cancer subtypes may identify a subset of patients that may benefit from PI3K inhibitor therapy, however, the relative expression and activation of AKT1 may also impact on therapeutic decision making.

EXPERIMENTAL PROCEDURES

MDA-MB-231 and Hs578T Cell Culture

MDA-MB-231 (ATCC) and MDA-MB-231-luc cells (Dr. John Price) were maintained in Dulbecco's modified Eagle's medium (DMEM) supplemented with 10% fetal calf serum (FCS) (Invitrogen) (growth media). Hs578T cells were maintained in RPMI 1640 supplemented with 10% FCS, 10 μg/ml insulin (Sigma), and 20 mM HEPES.

Transwell Cell Migration Assays

Cells were seeded at 5×10^4 per well in the top chamber of a Transwell in serum-free DMEM in duplicate. Cells were allowed to migrate toward DMEM, 10% FCS for 3 hr (MDA-MB-231) or 24 hr (*PyMT;Pipp* tumor cell lines) at 37°C. For AKT inhibitor studies, 2.5 μM AktX was added to both the top and bottom chambers of the Transwell. Non-migrated cells were removed from the upper chamber surface with a cotton swab, and cells that had migrated to the underside of the upper chamber were fixed and stained using a Diff-Quick Staining Kit (Lab Aids P/L). Cells were imaged using a ×20 objective on an Olympus CKX41 light microscope. The average number of migrated cells was scored from 12 fields/Transwell.

Generation of *Pipp*$^{-/-}$ Mice and *PyMT;Pipp*$^{-/-}$ Mice

Details of the mouse strains generated can be found in the Supplemental Information. All procedures involving mice were conducted in accordance with National Health and Medical Research Council (NHMRC) regulations on the use and care of experimental animals and were approved by the Monash University Animal Ethics Committee (SOBSB/2006/57 and SOBSB/2008/14).

Statistical Analysis

TissueScan Breast Cancer Arrays were analyzed by a two-tailed Mann-Whitney test. Tumor growth in *PyMT;Pipp* mice and phosphoinositide signals were analyzed by two-way ANOVA with Bonferroni post-test. Transwell cell migration assays, anchorage independent cell growth assays, and *Akt* shRNA western blots were assessed by one-way ANOVA with Tukeys multiple comparisons test. Droplet digital PCR assays were analyzed by two-way ANOVA with Bonferroni post-test. All other p values were determined using a Student's t test.

Further or detailed experimental procedures are described in the Supplemental Information.

SUPPLEMENTAL INFORMATION

Supplemental Information includes Supplemental Experimental Procedures and six figures and can be found with this article online at http://dx.doi.org/10.1016/j.ccell.2015.07.003.

REFERENCES

Allione, F., Eisinger, F., Parc, P., Noguchi, T., Sobol, H., and Birnbaum, D. (1998). Loss of heterozygosity at loci from chromosome arm 22Q in human sporadic breast carcinomas. Int. J. Cancer 75, 181–186.

Arboleda, M.J., Lyons, J.F., Kabbinavar, F.F., Bray, M.R., Snow, B.E., Ayala, R., Danino, M., Karlan, B.Y., and Slamon, D.J. (2003). Overexpression of AKT2/protein kinase Bbeta leads to up-regulation of β1 integrins, increased invasion, and metastasis of human breast and ovarian cancer cells. Cancer Res. 63, 196–206.

Astle, M.V., Horan, K.A., Ooms, L.M., and Mitchell, C.A. (2007). The inositol polyphosphate 5-phosphatases: traffic controllers, waistline watchers and tumour suppressors? Biochem. Soc. Symp. 74, 161–181.

Astrinidis, A., Cash, T.P., Hunter, D.S., Walker, C.L., Chernoff, J., and Henske, E.P. (2002). Tuberin, the tuberous sclerosis complex 2 tumor suppressor gene product, regulates Rho activation, cell adhesion and migration. Oncogene 21, 8470–8476.

Cancer Genome Atlas Network (2012). Comprehensive molecular portraits of human breast tumours. Nature 490, 61–70.

Carpten, J.D., Faber, A.L., Horn, C., Donoho, G.P., Briggs, S.L., Robbins, C.M., Hostetter, G., Boguslawski, S., Moses, T.Y., Savage, S., et al. (2007). A transforming mutation in the pleckstrin homology domain of AKT1 in cancer. Nature 448, 439–444.

Castells, A., Gusella, J.F., Ramesh, V., and Rustgi, A.K. (2000). A region of deletion on chromosome 22q13 is common to human breast and colorectal cancers. Cancer Res. 60, 2836–2839.

Chabottaux, V., and Noel, A. (2007). Breast cancer progression: insights into multifaceted matrix metalloproteinases. Clin. Exp. Metastasis 24, 647–656.

Chew, C.L., Lunardi, A., Gulluni, F., Ruan, D.T., Chen, M., Salmena, L.P.D., Nishino, M., Papa, A., Ng, C., Fung, J., et al. (2015). In vivo role of INPP4B in tumor and metastasis suppression through regulation of PI3K/AKT signaling at endosomes. Cancer Discov. 5, 740–751.

Chin, Y.R., and Toker, A. (2009). Function of Akt/PKB signaling to cell motility, invasion and the tumor stroma in cancer. Cell. Signal. 21, 470–476.

Chin, Y.R., Yoshida, T., Marusyk, A., Beck, A.H., Polyak, K., and Toker, A. (2014a). Targeting Akt3 signaling in triple-negative breast cancer. Cancer Res. 74, 964–973.

Chin, Y.R., Yuan, X., Balk, S.P., and Toker, A. (2014b). PTEN-deficient tumors depend on AKT2 for maintenance and survival. Cancer Discov. 4, 942–955.

Creighton, C.J. (2007). A gene transcription signature of the Akt/mTOR pathway in clinical breast tumors. Oncogene 26, 4648–4655.

Davies, E.M., Kong, A.M., Tan, A., Gurung, R., Sriratana, A., Bukczynska, P.E., Ooms, L.M., McLean, C.A., Tiganis, T., and Mitchell, C.A. (2014). Differential SKIP expression in PTEN-deficient glioblastoma regulates cellular proliferation and migration. Oncogene 4, 3711–3727.

Denley, A., Gymnopoulos, M., Kang, S., Mitchell, C., and Vogt, P.K. (2009). Requirement of phosphatidylinositol(3,4,5)trisphosphate in phosphatidylinositol 3-kinase-induced oncogenic transformation. Mol. Cancer Res. 7, 1132–1138.

Dillon, R.L., Marcotte, R., Hennessy, B.T., Woodgett, J.R., Mills, G.B., and Muller, W.J. (2009). Akt1 and akt2 play distinct roles in the initiation and metastatic phases of mammary tumor progression. Cancer Res. 69, 5057–5064.

Dumont, A.G., Dumont, S.N., and Trent, J.C. (2012). The favorable impact of PIK3CA mutations on survival: an analysis of 2587 patients with breast cancer. Chin. J. Cancer 31, 327–334.

Dyson, J., Fedele, C., Davies, E., Becanovic, J., and Mitchell, C. (2012). Phosphoinositide phosphatases: just as important as the kinases. In Phosphoinositides I: Enzymes of Synthesis and Degradation, T. Balla, M. Wymann, and J.D. York, eds. (Springer Netherlands), pp. 215–279.

Ellsworth, R.E., Ellsworth, D.L., Lubert, S.M., Hooke, J., Somiari, R.I., and Shriver, C.D. (2003). High-throughput loss of heterozygosity mapping in 26 commonly deleted regions in breast cancer. Cancer Epidemiol. Biomarkers Prev. 12, 915–919.

Gershtein, E.S., Scherbakov, A.M., Shatskaya, V.A., Kushlinsky, N.E., and Krasil'nikov, M.A. (2007). Phosphatidylinositol 3-kinase/AKT signalling pathway components in human breast cancer: clinicopathological correlations. Anticancer Res. 27 (4A), 1777–1782.

Grell, P., Fabian, P., Khoylou, M., Radova, L., Slaby, O., Hrstka, R., Vyzula, R., Hajduch, M., and Svoboda, M. (2012). Akt expression and compartmentalization in prediction of clinical outcome in HER2-positive metastatic breast cancer patients treated with trastuzumab. Int. J. Oncol. 41, 1204–1212.

Gruvberger, S., Ringnér, M., Chen, Y., Panavally, S., Saal, L.H., Borg A, Fernö, M., Peterson, C., and Meltzer, P.S. (2001). Estrogen receptor status in breast cancer is associated with remarkably distinct gene expression patterns. Cancer Res. 61, 5979–5984.

Guy, C.T., Cardiff, R.D., and Muller, W.J. (1992). Induction of mammary tumors by expression of polyomavirus middle T oncogene: a transgenic mouse model for metastatic disease. Mol. Cell. Biol. 12, 954–961.

Györffy, B., Lanczky, A., Eklund, A.C., Denkert, C., Budczies, J., Li, Q., and Szallasi, Z. (2010). An online survival analysis tool to rapidly assess the effect of 22,277 genes on breast cancer prognosis using microarray data of 1,809 patients. Breast Cancer Res. Treat. 123, 725–731.

Hollander, M.C., Blumenthal, G.M., and Dennis, P.A. (2011). PTEN loss in the continuum of common cancers, rare syndromes and mouse models. Nat. Rev. Cancer 11, 289–301.

Hutchinson, J., Jin, J., Cardiff, R.D., Woodgett, J.R., and Muller, W.J. (2001). Activation of Akt (protein kinase B) in mammary epithelium provides a critical cell survival signal required for tumor progression. Mol. Cell. Biol. 21, 2203–2212.

Hutchinson, J.N., Jin, J., Cardiff, R.D., Woodgett, J.R., and Muller, W.J. (2004). Activation of Akt-1 (PKB-α) can accelerate ErbB-2-mediated mammary tumorigenesis but suppresses tumor invasion. Cancer Res. 64, 3171–3178.

Iida, A., Kurose, K., Isobe, R., Akiyama, F., Sakamoto, G., Yoshimoto, M., Kasumi, F., Nakamura, Y., and Emi, M. (1998). Mapping of a new target region of allelic loss to a 2-cM interval at 22q13.1 in primary breast cancer. Genes Chromosomes Cancer 21, 108–112.

Ivetac, I., Gurung, R., Hakim, S., Horan, K.A., Sheffield, D.A., Binge, L.C., Majerus, P.W., Tiganis, T., and Mitchell, C.A. (2009). Regulation of PI(3)K/Akt signalling and cellular transformation by inositol polyphosphate 4-phosphatase-1. EMBO Rep. 10, 487–493.

Jezierska, A., and Motyl, T. (2009). Matrix metalloproteinase-2 involvement in breast cancer progression: a mini-review. Med. Sci. Monit. 15, RA32–RA40.

Ju, X., Katiyar, S., Wang, C., Liu, M., Jiao, X., Li, S., Zhou, J., Turner, J., Lisanti, M.P., Russell, R.G., et al. (2007). Akt1 governs breast cancer progression in vivo. Proc. Natl. Acad. Sci. USA 104, 7438–7443.

Kalinsky, K., Jacks, L.M., Heguy, A., Patil, S., Drobnjak, M., Bhanot, U.K., Hedvat, C.V., Traina, T.A., Solit, D., Gerald, W., et al. (2009). PIK3CA mutation associates with improved outcome in breast cancer. Clin. Cancer Res. 15, 5049–5059.

Kim, M.S., Jeong, E.G., Yoo, N.J., and Lee, S.H. (2008). Mutational analysis of oncogenic AKT E17K mutation in common solid cancers and acute leukaemias. Br. J. Cancer 98, 1533–1535.

Larkins, T.L., Nowell, M., Singh, S., and Sanford, G.L. (2006). Inhibition of cyclooxygenase-2 decreases breast cancer cell motility, invasion and matrix metalloproteinase expression. BMC Cancer 6, 181.

Li, G., Robinson, G.W., Lesche, R., Martinez-Diaz, H., Jiang, Z., Rozengurt, N., Wagner, K.-U., Wu, D.-C., Lane, T.F., Liu, X., et al. (2002). Conditional loss of PTEN leads to precocious development and neoplasia in the mammary gland. Development 129, 4159–4170.

Lin, E.Y., Jones, J.G., Li, P., Zhu, L., Whitney, K.D., Muller, W.J., and Pollard, J.W. (2003). Progression to malignancy in the polyoma middle T oncoprotein mouse breast cancer model provides a reliable model for human diseases. Am. J. Pathol. 163, 2113–2126.

Lin, C., Liu, A., Zhu, J., Zhang, X., Wu, G., Ren, P., Wu, J., Li, M., Li, J., and Song, L. (2014). miR-508 sustains phosphoinositide signalling and promotes aggressive phenotype of oesophageal squamous cell carcinoma. Nat. Commun. 5, 4620.

Liu, H., Radisky, D.C., Nelson, C.M., Zhang, H., Fata, J.E., Roth, R.A., and Bissell, M.J. (2006). Mechanism of Akt1 inhibition of breast cancer cell invasion reveals a protumorigenic role for TSC2. Proc. Natl. Acad. Sci. USA *103*, 4134–4139.

Liu, P., Cheng, H., Santiago, S., Raeder, M., Zhang, F., Isabella, A., Yang, J., Semaan, D.J., Chen, C., Fox, E.A., et al. (2011). Oncogenic PIK3CA-driven mammary tumors frequently recur via PI3K pathway-dependent and PI3K pathway-independent mechanisms. Nat. Med. *17*, 1116–1120.

Ma, C.X., and Ellis, M.J. (2013). The Cancer Genome Atlas: clinical applications for breast cancer. Oncology, (Williston Park, NY) *27*, 1263–1269, 1274–1279.

Maroulakou, I.G., Oemler, W., Naber, S.P., and Tsichlis, P.N. (2007). Akt1 ablation inhibits, whereas Akt2 ablation accelerates, the development of mammary adenocarcinomas in mouse mammary tumor virus (MMTV)-ErbB2/neu and MMTV-polyoma middle T transgenic mice. Cancer Res. *67*, 167–177.

Meyer, D.S., Brinkhaus, H., Müller, U., Müller, M., Cardiff, R.D., and Bentires-Alj, M. (2011). Luminal expression of PIK3CA mutant H1047R in the mammary gland induces heterogeneous tumors. Cancer Res. *71*, 4344–4351.

Miller, T.W., Rexer, B.N., Garrett, J.T., and Arteaga, C.L. (2011). Mutations in the phosphatidylinositol 3-kinase pathway: role in tumor progression and therapeutic implications in breast cancer. Breast Cancer Res. *13*, 224.

Ooms, L.M., Fedele, C.G., Astle, M.V., Ivetac, I., Cheung, V., Pearson, R.B., Layton, M.J., Forrai, A., Nandurkar, H.H., and Mitchell, C.A. (2006). The inositol polyphosphate 5-phosphatase, PIPP, Is a novel regulator of phosphoinositide 3-kinase-dependent neurite elongation. Mol. Biol. Cell *17*, 607–622.

Ooms, L.M., Horan, K.A., Rahman, P., Seaton, G., Gurung, R., Kethesparan, D.S., and Mitchell, C.A. (2009). The role of the inositol polyphosphate 5-phosphatases in cellular function and human disease. Biochem. J. *419*, 29–49.

Osborne, R.J., and Hamshere, M.G. (2000). A genome-wide map showing common regions of loss of heterozygosity/allelic imbalance in breast cancer. Cancer Res. *60*, 3706–3712.

Pang, B., Cheng, S., Sun, S.-P., An, C., Liu, Z.-Y., Feng, X., and Liu, G.-J. (2014). Prognostic role of PIK3CA mutations and their association with hormone receptor expression in breast cancer: a meta-analysis. Sci. Rep. *4*, 6255.

Park, B.K., Zeng, X., and Glazer, R.I. (2001). Akt1 induces extracellular matrix invasion and matrix metalloproteinase-2 activity in mouse mammary epithelial cells. Cancer Res. *61*, 7647–7653.

Sabine, V.S., Crozier, C., Brookes, C.L., Drake, C., Piper, T., van de Velde, C.J.H., Hasenburg, A., Kieback, D.G., Markopoulos, C., Dirix, L., et al. (2014). Mutational analysis of PI3K/AKT signaling pathway in tamoxifen exemestane adjuvant multinational pathology study. J. Clin. Oncol. *32*, 2951–2958.

Schwertfeger, K.L., Richert, M.M., and Anderson, S.M. (2001). Mammary gland involution is delayed by activated Akt in transgenic mice. Mol. Endocrinol. *15*, 867–881.

Stål, O., Pérez-Tenorio, G., Akerberg, L., Olsson, B., Nordenskjöld, B., Skoog, L., and Rutqvist, L.E. (2003). Akt kinases in breast cancer and the results of adjuvant therapy. Breast Cancer Res. *5*, R37–R44.

Sun, M., Wang, G., Paciga, J.E., Feldman, R.I., Yuan, Z.Q., Ma, X.L., Shelley, S.A., Jove, R., Tsichlis, P.N., Nicosia, S.V., and Cheng, J.Q. (2001). AKT1/PKBalpha kinase is frequently elevated in human cancers and its constitutive activation is required for oncogenic transformation in NIH3T3 cells. Am. J. Pathol. *159*, 431–437.

Tikoo, A., Roh, V., Montgomery, K.G., Ivetac, I., Waring, P., Pelzer, R., Hare, L., Shackleton, M., Humbert, P., and Phillips, W.A. (2012). Physiological levels of Pik3ca[H1047R] mutation in the mouse mammary gland results in ductal hyperplasia and formation of ERα-positive tumors. PLoS ONE *7*, e36924.

Toker, A. (2012). Achieving specificity in Akt signaling in cancer. Adv. Biol. Regul. *52*, 78–87.

van 't Veer, L.J., Dai, H., van de Vijver, M.J., He, Y.D., Hart, A.A., Mao, M., Peterse, H.L., van der Kooy, K., Marton, M.J., Witteveen, A.T., et al. (2002). Gene expression profiling predicts clinical outcome of breast cancer. Nature *415*, 530–536.

Voduc, K.D., Cheang, M.C.U., Tyldesley, S., Gelmon, K., Nielsen, T.O., and Kennecke, H. (2010). Breast cancer subtypes and the risk of local and regional relapse. J. Clin. Oncol. *28*, 1684–1691.

Ye, Y., Jin, L., Wilmott, J.S., Hu, W.L., Yosufi, B., Thorne, R.F., Liu, T., Rizos, H., Yan, X.G., Dong, L., et al. (2013). PI(4,5)P2 5-phosphatase A regulates PI3K/Akt signalling and has a tumour suppressive role in human melanoma. Nat. Commun. *4*, 1508.

Yoeli-Lerner, M., Yiu, G.K., Rabinovitz, I., Erhardt, P., Jauliac, S., and Toker, A. (2005). Akt blocks breast cancer cell motility and invasion through the transcription factor NFAT. Mol. Cell *20*, 539–550.

Yoeli-Lerner, M., Chin, Y.R., Hansen, C.K., and Toker, A. (2009). Akt/protein kinase b and glycogen synthase kinase-3beta signaling pathway regulates cell migration through the NFAT1 transcription factor. Mol. Cancer Res. *7*, 425–432.

Young, C.D., Nolte, E.C., Lewis, A., Serkova, N.J., and Anderson, S.M. (2008). Activated Akt1 accelerates MMTV-c-ErbB2 mammary tumourigenesis in mice without activation of ErbB3. Breast Cancer Res. *10*, R70.

Yuan, T.L., and Cantley, L.C. (2008). PI3K pathway alterations in cancer: variations on a theme. Oncogene *27*, 5497–5510.

Zhang, H.-Y., Liang, F., Jia, Z.-L., Song, S.-T., and Jiang, Z.-F. (2013). PTEN mutation, methylation and expression in breast cancer patients. Oncol. Lett. *6*, 161–168.